

## REPORT 1354

# EFFECT OF CHORD SIZE ON WEIGHT AND COOLING CHARACTERISTICS OF AIR-COOLED TURBINE BLADES<sup>1</sup>

By JACK B. ESGAR, EUGENE F. SCHUM, and ARTHUR N. CURREN

### SUMMARY

*An analysis has been made to determine the effect of chord size on the weight and cooling characteristics of shell-supported, air-cooled gas-turbine blades. In uncooled turbines with solid blades, the general practice has been to design turbines with high aspect ratio (small blade chord) to achieve substantial turbine weight reduction. With air-cooled blades, this study shows that turbine blade weight is affected to a much smaller degree by the size of the blade chord.*

*The heat-transfer analysis shows that considerable saving in coolant flow is possible by utilizing a smaller number of large-chord blades rather than a larger number of small-chord blades with constant blade solidity. Generally, turbines with a blade chord of only 1 inch require about twice as much coolant as turbines with 3-inch-chord blades for a turbine-inlet temperature of 2500° R. As the blade chord is reduced below 1 inch, as it might be in small-diameter engines, the coolant-flow requirements increase very rapidly. The coolant flow required for a blade with ½-inch chord may be more than twice that required for a 1-inch-chord blade. In addition to the high coolant flows necessary, the small-chord blades are often unable to pass the required coolant flow at the pressure levels encountered in engine operation. Although this investigation was conducted specifically on corrugated-insert blades, the trends of the results are believed to be general. The study shows that, in air-cooled-turbine design, efforts should be made to use blades with as large a chord as appears feasible with regard to disk stress and aerodynamics.*

### INTRODUCTION

Turbine blade chord is an important consideration in the design of uncooled turbines, primarily because of its effect on turbine weight. This investigation was conducted to determine how blade chord affects the weight and cooling characteristics of air-cooled turbines. In general, the number of blades in a turbine can vary considerably without significantly affecting the turbine performance as long as the blade solidity (ratio of chord to pitch) is maintained constant. For solid uncooled turbine blades, the total airfoil weight is inversely proportional to the number of blades in the turbine (directly proportional to chord) for constant solidity. Since aerodynamic performance is only slightly affected but weight is significantly affected by the number of blades, it has been common practice among manufacturers of uncooled turbines to use a large number of short-chord high-aspect-ratio blades

in their turbines. With the introduction of cooling into the turbine, some of the old rules are no longer valid, and a new look is required to determine optimum blade sizes.

In order to permit increases in turbine-inlet temperature on the order of 500° to 1000° R, it is necessary to extend coolant passages well into the blade leading and trailing edges. The trailing-edge coolant passages usually cause a thickening of the trailing edge and increased gas-passage blockage for each blade. This gas-passage blockage results in an aerodynamic performance loss. The required trailing-edge thickness for air-cooled blades is almost independent of blade size. A method of reducing the total gas blockage for the turbine is to reduce the number of blades and increase the chord to maintain solidity. As a result, the optimum number of blades with respect to aerodynamic performance may therefore decrease as trailing-edge thickness is increased.

Other factors may also suggest the use of a smaller number of larger-chord blades in air-cooled turbines. It is easier to build the required internal surface area into larger blades, and the total coolant-passage flow area for the turbine is almost directly proportional to chord size (same as weight being proportional to chord for solid uncooled blades), so that, for a given flow rate, pressure losses should be smaller when the chord is increased. In addition, total airfoil weight for blades with a portion of the interior hollowed out is no longer directly proportional to the chord for constant solidity. If the airfoils were thin hollow shells, the total airfoil weight for constant-solidity turbines would almost be independent of chord size.

In order to obtain a better understanding of the effects of chord size on air-cooled turbine blade weight, cooling effectiveness, and cooling-air pressure losses, an analytical study was made of these effects for corrugated-insert blades with chords varying from ½ to 3½ inches. In these studies two-stage turbine engines were considered, with turbine diameters varying from 15 to 35 inches, so that the turbine blade aspect ratios varied from approximately 1 to 4 for the range of chords considered. Required coolant flow and pressure losses were calculated for an engine with a sea-level compressor pressure ratio of 10 flying at a Mach number of 2.0 at 50,000 feet. While these results may not be completely general, the trends should be indicative of the effect of turbine blade chord size for a wide range of application.

<sup>1</sup> Supersedes NACA Technical Note 3923 by Jack B. Esgar, Eugene F. Schum, and Arthur N. Curren, 1957.

## SYMBOLS

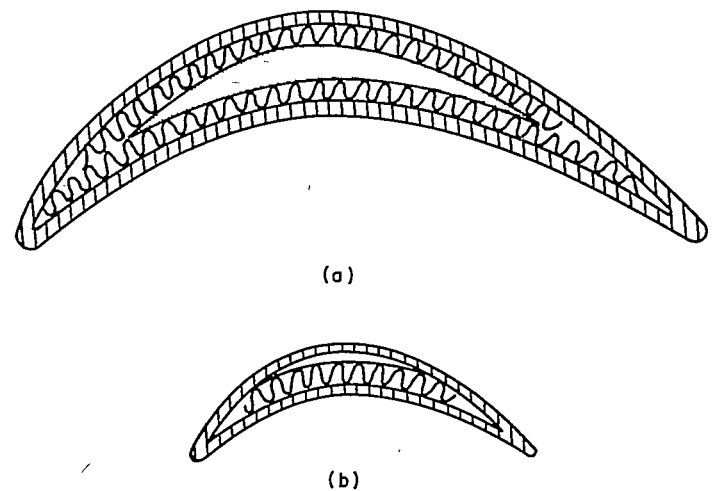
$A$	cross-sectional metal area, sq in.
$A_{ft}$	flow area, sq ft
$\mathcal{A}$	turbine blade aspect ratio
$C_f$	friction coefficient
$c$	turbine blade chord, ft
$c_p$	specific heat at constant pressure, Btu/(lb) (°R)
$D$	diameter, ft
$E$	pumping work, Btu/lb
$\bar{F}$	constant, function of blade transition ratio and Euler number
$\mathcal{F}$	centrifugal force, lb
$g$	acceleration due to gravity, ft/sec <sup>2</sup>
$h_i$	effective inside heat-transfer coefficient, Btu/(sec) (sq ft) (°R)
$h_t$	blade-to-coolant heat-transfer coefficient, Btu/(sec) (sq ft) (°R)
$h_o$	gas-to-blade heat-transfer coefficient, Btu/(sec) (sq ft) (°R)
$J$	mechanical equivalent of heat, ft-lb/Btu
$K_1, K_2, \dots K_s$	constants
$k$	thermal conductivity, Btu/(sec) (ft) (°R)
$L$	effective fin length, ft
$l$	blade perimeter, ft
$M$	mass, (lb) (sec <sup>2</sup> )/ft
$m$	distance between fins, ft
$Nu$	Nusselt number
$P'$	relative total pressure, lb/sq ft abs
$Pr$	Prandtl number
$p$	static pressure, lb/sq ft abs
$q$	heat flow, Btu/sec
$Re$	Reynolds number
$r$	radius from center of rotation, ft
$S$	surface area, sq ft
$T'$	relative total temperature, °R
$t$	static temperature, °R
$U_t$	tip speed, ft/sec
$w$	flow rate, lb/sec
$x$	distance from blade root, ft
$Y$	corrugation amplitude, in.
$z$	exponent, function of blade transition ratio and Euler number
$\alpha$	coolant-passage aspect ratio, ratio of corrugation amplitude to half corrugation pitch
$\Gamma$	metal density, lb/cu in.
$\mu$	viscosity, (lb) (sec)/(sq ft)
$\sigma$	stress, psi
$\tau$	fin thickness, ft
$\phi$	$\sqrt{2h_i/k_r\tau}$
$\omega$	angular velocity, radians/sec
Subscripts:	
$a$	cooling air
$b$	blade, or based on blade temperature
$c$	corrugations
$e$	effective
$g$	gas
$h$	hub
$i$	inside
$o$	outside

$T$	turbine
$t$	tip
$z$	local condition at $z$ feet above blade root

ANALYSIS AND PROCEDURE  
AIRFOIL WEIGHT AND SURFACE AREAS

The internal surface area per unit length of span of air-cooled turbine blades depends upon the aerodynamic profile of the blade, the blade chord, and the shell thickness, as well as the type of internal configuration. As the blade chord is varied, it generally is not possible to scale the blade directly to make the ratio of internal to external surface area remain constant. There are several reasons for this. First, there are minimum practical dimensions with regard to strength and fabrication. It is possible to vary shell thickness somewhat, but there are minimum thicknesses that depend on impact loads that the shell must withstand from foreign objects in the gas stream such as sand and carbon flakes. Minimum thicknesses of both the shell and internal configuration are determined by structural rigidity and by the effect of braze penetration for configurations that rely on brazing. In addition, the individual coolant-passage size can be reduced only so far and then the cooling-air pressure losses may become exorbitant or the passages may become plugged by brazing during fabrication or by small particles of foreign matter in the cooling air. For these reasons, both large and small blades may have an internal configuration where each passage has the same dimensions.

A type of air-cooled turbine blade that offers considerable potentiality for permitting substantial increases in turbine-inlet temperature with moderate cooling-airflow requirements is the corrugated-insert blade such as shown in figure 1(a). In this type of blade, corrugations of uniform amplitude are brazed to the inside surfaces of the blade shell. The best corrugation geometry is generally one that provides a maximum of surface area within pressure-drop limitations. This best corrugation is usually independent of blade chord as long as it can be placed inside the blade cavity, but the relative chordwise length of this corrugation is very much dependent upon the blade chord, as illustrated in figure 1



(a) Typical corrugated-insert blade.  
(b) Effect of placing corrugation in small-chord blade.

FIGURE 1.—Effect of blade chord on air-cooled blade inside heat-transfer surface area.

for two blades of the same profile but with different chord lengths.

The ratio of internal to external surface area gives an indication of blade-cooling effectiveness. A practical method of determining how chord size affects the internal surface area is to make layouts of each blade to be investigated. This method was used in this report by using an assumed outside blade profile at the mean section shown in figure 1, where the maximum blade thickness is approximately 15 percent of the chord. The coolant passage was assumed to be uniform from root to tip. The outside profile changed slightly to permit taper in the blade shell. These assumptions result in a slight approximation, because in actual practice the blade profile will change along the blade span more than considered herein, but it is possible with proper design to maintain internal surface area approximately constant from root to tip. In all cases it was assumed that metal corrugations and the sheet-metal island in the center of the blade were of uniform thickness along the span. The corrugations were assumed to be 0.005 inch thick, and the island sheet metal 0.010 inch thick. The pitch of the corrugations was assumed to be 0.050 inch, and the amplitude was varied from 0.030 to 0.070 inch. This range of internal geometries has been found to have effective heat-transfer characteristics from a study of corrugations by the method of reference 1. The chordwise length of the corrugations in each blade size being known from layouts, the surface area and the cross-sectional area were calculated from relations given in reference 1. The blade shell, including leading- and trailing-edge portions where there were no corrugations, was also included in these calculations. The blade weight was calculated from the cross-sectional area using a metal density of 0.3 pound per cubic inch.

For a linear variation in metal cross-sectional area from root to tip of turbine blades, an expression for the centrifugal-stress distribution in the blades can be derived in the following manner. The cross-sectional-area distribution along the span can be expressed by

$$\frac{A-A_x}{A_t-A_x} = \frac{r-r_x}{r_t-r_x} \quad (1)$$

or

$$A = A_x \left[ 1 - \frac{r-r_x}{r_t-r_x} \left( 1 - \frac{A_t}{A_x} \right) \right] \quad (2)$$

where  $r$  and  $A$  are variables. The stress is obtained from

$$\sigma_x = \frac{\mathcal{F}_x}{A_x} = \int_{r_x}^{r_t} \frac{r \omega^2}{A_x} dM \quad (3)$$

where

$$dM = \frac{12 \Gamma A dr}{g} \quad (4)$$

and the constant 12 is a conversion from feet to inches. Combining equations (2) to (4) and integrating give the following expression:

$$\sigma_x = \frac{12 \omega^2 r_x^2 \Gamma}{g} \left\{ \frac{1}{2} \left[ 1 - \left( \frac{r_x}{r_t} \right)^2 \right] - \frac{1}{3} \frac{1 - \left( \frac{r_x}{r_t} \right)^3}{1 - \frac{r_x}{r_t}} \left( 1 - \frac{A_t}{A_x} \right) + \frac{1}{2} \left[ \frac{r_x}{r_t} + \left( \frac{r_x}{r_t} \right)^2 \right] \left( 1 - \frac{A_t}{A_x} \right) \right\} \quad (5)$$

If it is noted that  $U_t = \omega r$  and if terms are collected, equation (5) can be written

$$\sigma_x = \frac{12 U_t^2 \Gamma}{g} \left\{ \frac{1}{2} \left[ 1 - \left( \frac{r_x}{r_t} \right)^2 \right] - \frac{1}{6} \left[ 2 - \frac{r_x}{r_t} - \left( \frac{r_x}{r_t} \right)^2 \right] \left( 1 - \frac{A_t}{A_x} \right) \right\} \quad (5a)$$

By letting  $r_x = r_h$  and  $A_x = A_h$  in equation (5a), the centrifugal stress at the blade root can be calculated; and by multiplying both sides of equation (5a) by  $(1200/U_t)^2$  an equivalent root stress can be obtained. The resulting values of equivalent root stress  $\sigma(1200/U_t)^2$  are then, of course, the actual stresses for a tip speed of 1200 feet per second, which is a representative turbine speed. The stress values are presented in this manner so that they can be quickly converted to the stress that would result for any other tip speed of interest.

TABLE I.—TEMPERATURES, PRESSURES, AND OTHER CONDITIONS USED IN ANALYSIS

<i>Assigned conditions:</i>	
Engine compressor pressure ratio.....	10 at sea-level-static conditions; 6.3 at flight conditions
Flight altitude, ft.....	50,000
Flight Mach number.....	2.0
Turbine-inlet temp., °R.....	2500
Ram recovery pressure ratio.....	0.87
Compressor adiabatic efficiency.....	0.85
Turbine adiabatic efficiency.....	0.85
Relative Mach number of gas entering turbine.....	0.6
Mach number of gas at turbine exit.....	0.5
Max. centrifugal turbine blade root stress for taper factor of 0.7, psi.....	30,000
Second-turbine-stage hub-tip radius ratio.....	0.6
Turbine blade stress-ratio factor.....	1.0 (except fig. 11)
Turbine blade solidity at mean section (both stages).....	1.5
<i>Calculated conditions:</i>	
First-turbine-stage hub-tip radius ratio.....	0.73
Turbine tip speed (same for both stages), ft/sec.....	1095
Compressor-discharge temp. (blade root cooling-air temp. for most calculations), °R.....	1247
Compressor-discharge total pressure, lb/sq ft.....	10,420
Static gas pressure at blade tip, lb/sq ft.....	7340 (first-stage rotor); 4000 (second-stage rotor)
Effective gas temperature, °R.....	2390 (first-stage rotor); 2048 (second-stage rotor)
Constant $K_1$ in gas-to-blade heat-transfer coefficient, eq. (13).....	0.721 (first-stage rotor); 0.467 (second-stage rotor)

## TURBINE DESIGN

In order to make this analysis representative of conditions that might be encountered in cooled turbojet engines, a two-stage turbine was designed for an engine with a sea-level-static compressor pressure ratio of 10. The engine design point was taken for a flight Mach number of 2.0 at 50,000 feet. Heat-transfer calculations were also made for these conditions. The turbine was designed according to the methods in reference 2, and temperature and pressure conditions at various stations through the engine were calculated by means of reference 3. The assigned conditions and the resulting calculated conditions are listed in table I. The compressor pressure ratio of 6.3 at a flight Mach number of 2.0 would result from constant-mechanical-speed operation for an arbitrarily assumed compressor.

The assigned turbine conditions result in a conservative turbine design. In a conservative turbine there is considerable freedom in the choice of a blade profile. An assumed profile was used in this investigation that is believed to be typical of profiles that may be encountered in air-cooled engines. For the sake of simplicity, the same profile was used for both the first and second stages and for all chord lengths. The profile is shown in figure 1.

In order to investigate a representative range of engines, turbine diameters of 15, 25, and 35 inches were considered, with a corresponding size change in the rest of the engine. The turbine design was the same for all diameters, but of course the blade size varied with the diameter.

## BLADE COOLANT-FLOW REQUIREMENTS

The coolant-flow requirements for air-cooled turbine blades depend on the gas-to-blade heat-transfer coefficients, the blade temperature, the gas temperature, the coolant temperature at the blade base, and the coolant-passage geometry. In this analysis all these factors except the gas temperature vary for one reason or another. The calculation methods include each of these effects.

**Gas-to-blade heat-transfer coefficient.**—The average Nusselt number  $Nu$ , from which the average gas-to-blade heat-transfer coefficient  $h_o$  is obtained, can be found from the following correlation equation (ref. 4):

$$Nu = \bar{F}(Re)^z (Pr)^{1/3} \quad (6)$$

The reference length in the Nusselt and Reynolds numbers is  $l_o/\pi$ , and  $\bar{F}$  and  $z$  are functions of transition ratio and Euler number of the blade.

The Reynolds number in equation (6) may be written as

$$Re = \left( \frac{w_g \sqrt{T'_g}}{A_{f,g} P'_g} \right)_r \left( \frac{P'_g}{\sqrt{T'_g}} \right)_r \left( \frac{t_g}{t_b} \right) \left( \frac{l_o/\pi}{\mu_{g,b} g} \right) \quad (7)$$

By combining equations (6) and (7), the gas-to-blade heat-transfer coefficient can be expressed by

$$h_o = \left( \frac{\bar{F} k_{g,b}}{l_o/\pi} \right)^{1-z} \left[ \left( \frac{w_g \sqrt{T'_g}}{A_{f,g} P'_g} \right)_r \left( \frac{P'_g}{\sqrt{T'_g}} \right)_r \left( \frac{t_g}{t_b} \right) \left( \frac{1}{\mu_{g,b} g} \right) \right]^z Pr^{1/3} \quad (8)$$

The term  $w_g \sqrt{T'_g}/A_{f,g} P'_g$  is a function of gas Mach number and is essentially constant for Mach numbers between 0.7 and 1.0 (max. variation is about 9 percent). A Mach number of 0.7 is probably representative for most turbine designs; consequently,  $w_g \sqrt{T'_g}/A_{f,g} P'_g$  was evaluated from

reference 5 for that Mach number. For this investigation variations in gas pressure (due to altitude) and gas temperature were not considered. The gas fluid properties  $\mu_{g,b}$ ,  $k_{g,b}$ , and  $Pr$  can be written as a function of the blade temperature:

$$k_{g,b} = K_1 t_b^{0.85} \quad (9)$$

$$\mu_{g,b} = K_2 t_b^{0.7} \quad (10)$$

$$Pr \approx K_3 \quad (11)$$

The perimeter of the blade used in this analysis is  $2.34(c)$ . The perimeter can then be expressed in terms of the turbine tip diameter and the blade aspect ratio and hub-tip radius ratio as follows:

$$l_o = 2.34 \left( \frac{D_T}{2\mathcal{A}} \right) \left( 1 - \frac{r_h}{r_t} \right)_T \quad (12)$$

Substitution of equations (9) to (12) into equation (8) results in

$$h_o = \frac{K_4}{t_b^{1.7z-0.85}} \left( \frac{\mathcal{A}}{D_T} \right)^{1-z} \quad (13)$$

where  $K_4$  is a grouping of all the constant terms in equations (8) to (12).

In reference 6, ten blade profiles were analyzed, including both impulse and reaction blades. An average value of  $z$  for these ten blades is 0.70. Using the value of  $z$  for rotor blades, equation (13) becomes

$$h_o = \frac{K_4}{t_b^{0.34}} \left( \frac{\mathcal{A}}{D_T} \right)^{0.3} \quad (14)$$

Equations (13) and (14) can also be written

$$h_o = \frac{K_5}{t_b^{1.7z-0.85} c^{1-z}} = \frac{K_5}{t_b^{0.34} c^{0.3}} \quad (15)$$

In this investigation  $K_4$  was evaluated for each turbine stage; and then the variations in  $h_o$  with turbine diameter, blade aspect ratio, and blade temperature were calculated by use of equation (14). The turbine blade temperature  $t_b$  varies along the span because of heating of the cooling air.

**Blade-to-coolant heat-transfer coefficient.**—The boundary-layer flow inside air-cooled blades may be laminar, turbulent, or in transition. In laminar flow the heat-transfer correlation equation depends on the coolant-passage aspect ratio  $\alpha$  (ref. 7). For turbulent flow the Nusselt number can be written

$$\frac{Nu}{Re} = \frac{0.0199}{Re^{0.2}} \quad (16)$$

for a constant Prandtl number of 0.7 (ref. 8). In the transition region there is considerable uncertainty as to what the heat-transfer rates may be. In this analysis it was assumed that  $Nu/Re$  was a constant in this transition region and at the same value that results from turbulent flow for a Reynolds number of 8000. This transition region was assumed to extend down to a Reynolds number that would also result in the same  $Nu/Re$  in laminar flow. These heat-transfer correlations are represented graphically in figure 2 and mathematically in table II(a). In this manner the Reynolds number at which the flow changes from laminar to transition varies slightly with coolant-passage aspect ratio. The fluid properties of the coolant were based on the film temperature.

For finned coolant passages an effective heat-transfer coefficient  $h_f$  is required. The equation for evaluating  $h_f$  is given in reference 9 as

$$h_f = \frac{h_i}{m + \tau} \left( \frac{2 \tanh \phi L}{\phi} + m \right) \quad (17)$$

The effective coefficient is related to the inside coefficient by a function of the metal thermal conductivity and the ratio of the inside wetted perimeter to the outside perimeter. For the limiting case with infinite thermal conductivity, equation (17) becomes

$$\begin{aligned} h_f &= \frac{h_i}{m + \tau} (2L + m) \\ &= h_i \frac{l_i}{l_o} \end{aligned} \quad (18)$$

Equation (17) is evaluated for corrugated surfaces in reference 1 for corrugations having the same chordwise length as the outside surface that is exposed to the gas stream. In corrugated-insert blades it generally is not possible to extend the corrugations around the entire inside periphery of the blade. At the leading and trailing edges there are usually areas where there is not room to place the corrugations. For this reason, an evaluation of an entire turbine

blade using the value of  $h_f$  for a corrugated surface gives an optimistic answer. In this analysis it was assumed that the ratio of the effective coefficient for the entire blade to that for a corrugated surface was the same as the ratio of the inside and outside wetted perimeters for the entire blade to that for the corrugated surface, which is expressed in equation form as

$$\frac{(h_f)_b}{(h_f)_c} = \frac{\left(\frac{l_i}{l_o}\right)_b}{\left(\frac{l_i}{l_o}\right)_c} \quad (19)$$

where  $(h_f)_c$  is evaluated from reference 1 for the geometry used in the blade. This relation assumes that conduction effects are the same for the entire blade as they are for the corrugations.

**Spanwise blade temperature distribution.**—The local blade temperature  $t_{b,x}$  can be obtained from the following heat balance:

$$\frac{q}{S} = h_o(t_{g,s} - t_{b,x}) = (h_f)_b(t_{b,x} - T'_{a,x}) \quad (20)$$

where  $T'_{a,x}$  is the total cooling-air temperature relative to the blade at distance  $x$  from the blade root. This temperature is approximately equal to the effective air temperature at this

TABLE II.—EXPRESSIONS FOR BLADE COOLANT-PASSAGE NUSSELT NUMBER AND FRICTION COEFFICIENT

(a) Nusselt number

Corrugation amplitude, $Y$ , in.	Coolant-passage aspect ratio, $\alpha$	Reynolds number, $Re$	Nusselt number, $Nu$	Flow region
0.03–0.07	1.25–3.25	$\geq 8000$	$0.0199 Re^{0.3}$	Turbulent
0.07	3.25	1470–8000	$0.0033 Re$	Transition
		$\leq 1470$	4.85	Laminar
0.05	2.25	1280–8000	$0.0033 Re$	Transition
		$\leq 1280$	4.22	Laminar
0.03	1.25	1125–8000	$0.0033 Re$	Transition
		$\leq 1125$	3.72	Laminar

(b) Friction coefficient

Corrugation amplitude, $Y$ , in.	Coolant-passage aspect ratio, $\alpha$	Reynolds number, $Re$	Friction coefficient, $4C_{fr}$	Flow region
0.03–0.07	1.25–3.25	$\geq 8000$	$\frac{0.2935}{Re^{0.245}}$	Turbulent
0.07	3.25	2130–8000	0.03255	Transition
		$\leq 2130$	$\frac{69.2}{Re}$	Laminar
0.05	2.25	1970–8000	0.03255	Transition
		$\leq 1970$	$\frac{64.16}{Re}$	Laminar
0.03	1.25	1800–8000	0.03255	Transition
		$\leq 1800$	$\frac{58.65}{Re}$	Laminar

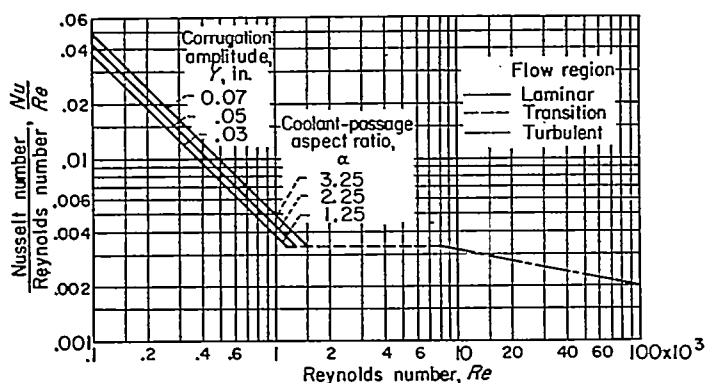


FIGURE 2.—Heat-transfer correlations for air-cooled-blade coolant passages.

point for subsonic Mach numbers. In this analysis the blade span was divided into ten equal increments, and a stepwise calculation procedure was used to calculate the temperature at each increment. To obtain the coolant-air temperature rise in each increment, the following heat balance was written:

$$q + w_a E = h_o l_o \Delta x (t_{s,e} - t_{b,z}) + w_a E = w_a c_{p,a} \Delta T'_a \quad (21)$$

where the pumping work  $E$  done on the cooling air over the increment  $\Delta x$  is

$$E = \frac{\omega^2 r_z \Delta x}{gJ} \quad (22)$$

Combining equations (21) and (22) results in

$$\Delta T'_a = \frac{h_o l_o \Delta x}{w_a c_{p,a}} (t_{s,e} - t_{b,z}) + \frac{\omega^2 r_z \Delta x}{gJ c_{p,a}} \quad (23)$$

The blade temperature used to evaluate film temperature and fluid properties and to calculate  $T'_a$  at each increment was that temperature calculated in the previous increment. The spanwise temperature variations in the blade are generally small enough that this approximation has little or no effect on the final results.

**Required cooling airflow.**—The allowable blade temperature distribution for turbine blades depends on the spanwise blade stress distribution, the stress-rupture properties of the blade material, and the stress-ratio factor, as discussed in reference 10. The required cooling airflow is that which results in a curve of calculated blade temperature against blade span that is tangent to a curve of allowable blade temperature. This cooling airflow was found by an iterative procedure. A maximum difference of  $2^\circ$  between the calculated and allowable blade temperature was permitted at the blade critical section (spanwise position where difference in calculated and allowable temperature is smallest) in determining the required cooling airflow.

#### BLADE PRESSURE LOSSES

The cooling-air pressure change through the turbine blades was calculated by the method of reference 5 by using the required cooling airflow from the calculations described previously. The blade was divided into five equal increments for these calculations. The friction coefficients used were the same as those that can be read from figure 3 of reference 1, using the same values of coolant-passage aspect ratio  $\alpha$  as shown in figure 2 of this report, except that in the transition

region the friction coefficient was assumed to be independent of Reynolds number in exactly the same manner as  $Nu/Re$  was assumed to be independent of transition Reynolds number in figure 2. Equations for the friction coefficient are given in table II(b) in terms of  $4C_f$  for convenience in the use of the calculation procedure of reference 5.

The cooling-air pressure at the blade base was assumed to be 90 percent of the compressor-discharge pressure, which allowed for duct losses and some losses in velocity head. It was assumed that, if the calculated coolant static pressure at the blade tip was equal to or greater than the static gas pressure at the blade tip and if the Mach number at the tip was subsonic, then the blade was satisfactory with respect to loss. The static gas pressure at the blade tip was calculated from the turbine velocity diagram that was required to drive the compressor at the assumed flight conditions.

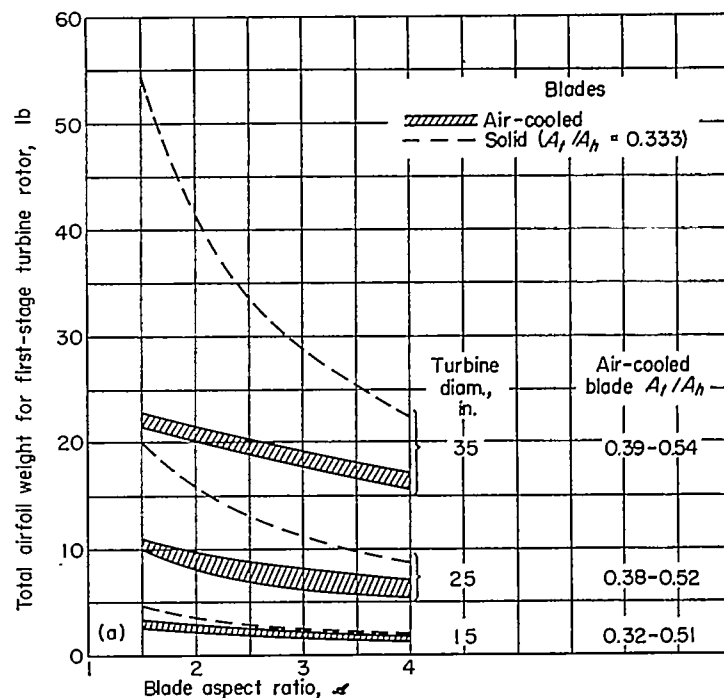
#### CALCULATION PROCEDURE

The entire calculation procedure for this analysis was set up in equation form, including the pressure-loss calculations and the relation between temperature and the 100-hour stress-rupture properties of A-286 alloy, the turbine blade material assumed for this analysis. The calculations were then made by an IBM 650 Magnetic Drum Data Processing Machine. Temperatures, pressures, and other conditions used in this analysis are listed in table I.

#### RESULTS AND DISCUSSION

##### AIRFOIL WEIGHT, STRESS, AND AREAS

**Weight.**—The total airfoil weights of all the rotor blades in a turbine stage are plotted against blade aspect ratio in figure 3 for both the first and second stages of the turbines for turbine diameters of 15, 25, and 35 inches. Although the



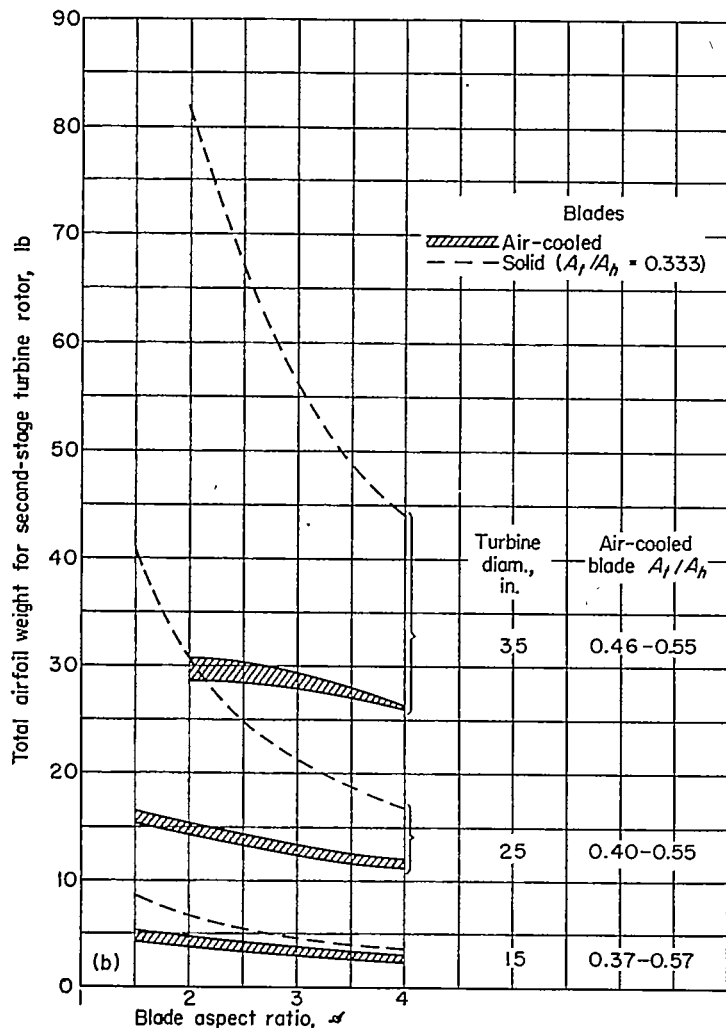
(a) First stage. Hub-tip radius ratio, 0.73.

FIGURE 3.—Variation of turbine blade airfoil weight with turbine diameter and blade aspect ratio.

analysis presented in this report is a study of the effects of blade chord on weight and cooling characteristics of air-cooled blades, it is more convenient to plot most of the results of the analysis against blade aspect ratio, because the range of aspect ratio is common to turbines of different diameters, while the range of chord size varies considerably for different diameter turbines.

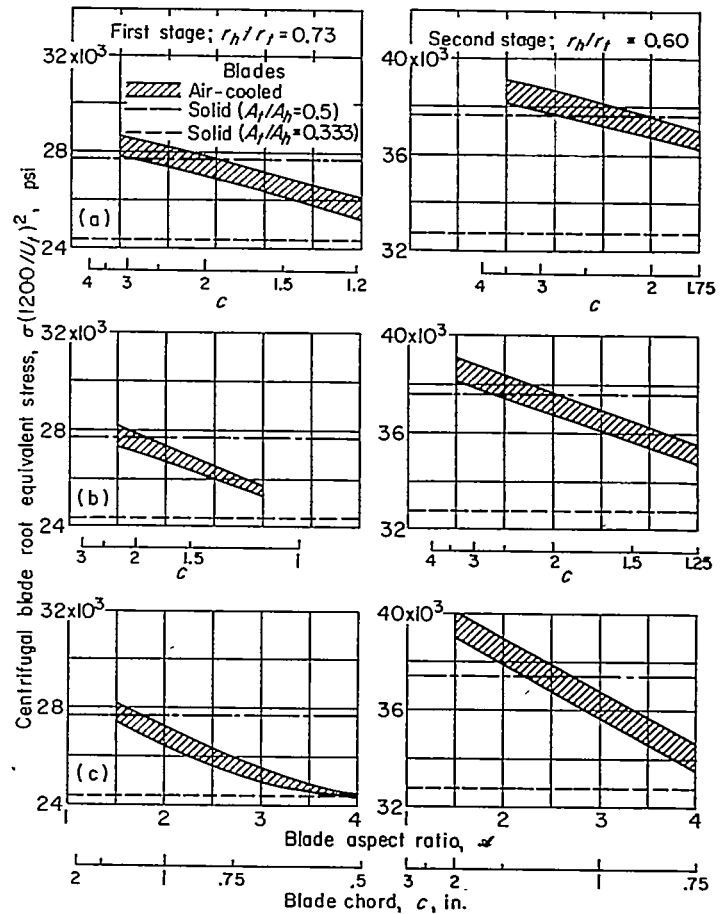
The weight of the air-cooled blades is represented by a shaded band. This band covers the range of weight values for the corrugation configurations considered herein. For turbine diameters of 25 and 35 inches, corrugation amplitudes of 0.03, 0.05, and 0.07 inch were considered, with an outside-shell thickness tapering from 0.045 inch at the root to 0.015 inch at the tip. For the 15-inch-diameter turbine, corrugation amplitudes of 0.03 and 0.05 inch were considered, with an outside-shell thickness tapering from 0.030 to 0.010 inch. Also shown in the figure are weights of solid uncooled blades having the same cross-sectional area at the root section of the blade and an aerodynamic taper of 3 to 1 from root to tip.

Two important conclusions may be drawn from figure 3. First, air-cooled blades are considerably lighter than solid blades having the same root profile, particularly for large



(b) Second stage. Hub-tip radius ratio, 0.60.

FIGURE 3.—Concluded. Variation of turbine blade airfoil weight with turbine diameter and blade aspect ratio.



(a) Turbine diameter, 35 inches.  
(b) Turbine diameter, 25 inches.  
(c) Turbine diameter, 15 inches.

FIGURE 4.—Air-cooled-turbine blade root stresses.

turbine diameters; and second, as aspect ratio (or chord) is varied, the total blade weight for the turbine is affected to a much smaller degree for air-cooled blades than for solid blades. Air-cooled blades of very low aspect ratio can be used, and the total turbine blade weight will still be lighter than with solid blades of high aspect ratio.

Airfoil weight does not show the entire picture with regard to turbine weight, however. The use of low-aspect-ratio blades requires alterations in the turbine disk design to support the longer chords. Generally, the longer chords will probably result in an increase in disk weight, so that the total turbine weight will increase with chord more than indicated in figure 3. Some types of disk structure, such as multiple disk wheels, may make it possible to increase chord with little or no increase in disk weight. An evaluation of disk weight, however, is beyond the scope of this report. A rather complete design study is required before representative variations in disk weight with blade chord can be made.

For constant-solidity turbines the total airfoil weight of solid blades varies inversely as the blade aspect ratio to the first power. (The individual blade weight varies inversely as the square of the aspect ratio.) In the study of air-cooled blades included herein, it was found that the total blade airfoil weight for the turbine varied inversely as the aspect ratio to a power varying between 0.1 and 0.65, depending on the turbine diameter. In general, the lower exponents ac-

company the large turbines (larger physical size of blades). For the 35-inch turbine the exponent was found to be about 0.1 for the second stage and about 0.3 for the first stage. For the 15-inch turbine the exponent was about 0.5 for the second stage and 0.65 for the first stage. The reason for this is obvious: With the smaller blades the shell and corrugations occupy a much larger portion of the cross-sectional area (the proportion of flow area decreases) than with the larger blades, so that the small blades more nearly approach the weight variation that occurs with solid blades.

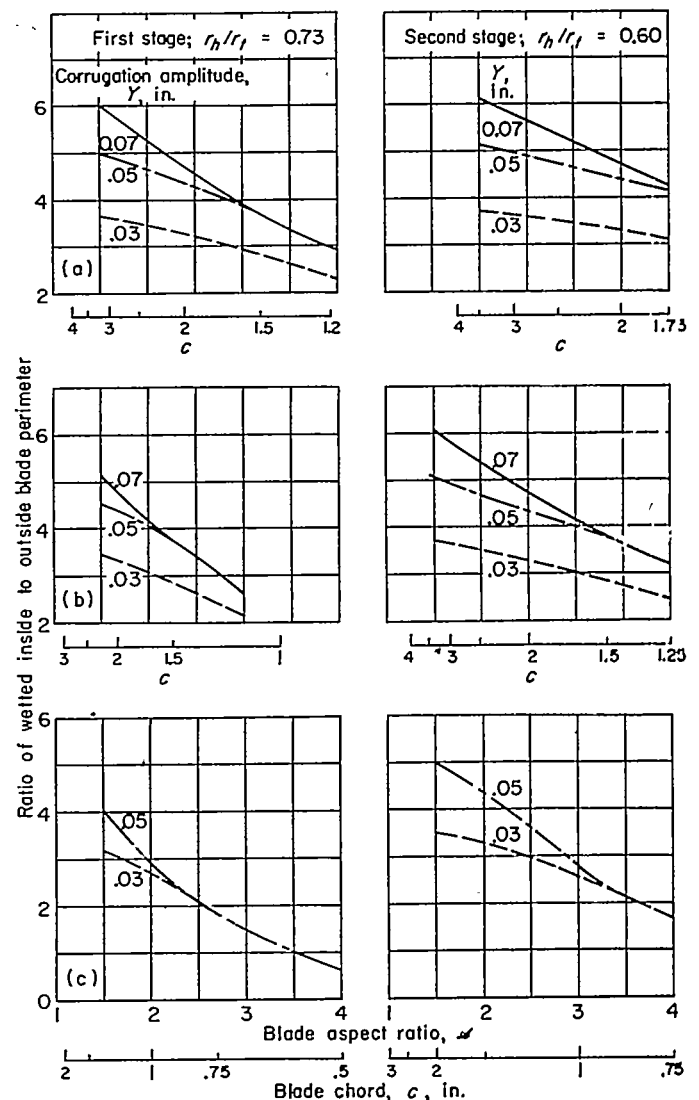
**Stress.**—From the root and tip cross-sectional areas that were determined for each blade configuration, the centrifugal root equivalent stress was calculated. The results are plotted against both blade aspect ratio and chord in figure 4. Subsequent figures are plotted in a similar manner. The stress values are presented as shaded bands, and they cover the same range of variables as discussed in connection with figure 3. For reference, root stresses are also shown for solid blades with tip-to-root area ratios of 0.5 and 0.333. The area ratios for the air-cooled blades vary with blade size. The shells of all the blades have an area ratio of 0.333, but the sheet metal making up the corrugations and islands in the blades is untapered. More corrugations can be installed in the larger-chord blades (low aspect ratio), which will help the heat-transfer characteristics; but the addition of this untapered sheet metal results in higher area ratios and thus higher root stresses.

Figure 4 shows that, generally, the centrifugal root stresses of corrugated-insert air-cooled blades will be of the same order of magnitude as those for solid blades with tip-to-root area ratios varying from 0.5 to 0.333. With low hub-tip radius ratios (on the order of 0.60 shown for the second stage) and for blade aspect ratios below 2.5 or 3, the air-cooled-blade stresses are likely to be higher than those for solid blades with an area ratio of 0.5. Figure 4 also compares tip-to-root cross-sectional-area ratios for air-cooled blades for various coolant-passage configurations, blade aspect ratios, and hub-tip radius ratios; however, a comparison based on root stress is probably of more general interest.

**Inside heat-transfer surface area.**—The amount of surface area that can be placed inside air-cooled turbine blades relative to the blade outside surface area affects the efficiency of blade-cooling. The ratio of the wetted perimeter on the inside of the blade to the outside perimeter is plotted in figure 5 as a function of blade chord and aspect ratio, turbine diameter, and corrugation amplitude  $Y$ . The ratio of perimeters can vary by as much as 7 to 1 as the blade chord is varied from about 1.5 to 0.5 inch (aspect ratio varying from 1.5 to 4) for the 15-inch-diameter turbine. For the larger turbine engines and the corresponding larger chords, the ratio of perimeters varies about 2 to 1 for the same range of aspect ratio. If it were possible to scale blade coolant passages geometrically, the ratio of inside to outside surface area would remain constant as chord is varied. As mentioned previously, this is not practical for turbine blades. The two sketches in figure 1 illustrate the problem involved when the blade chord is shortened and the same corrugation geometry is used for both blade sizes. The smaller sketch shows that it may not even be possible to attach separate

corrugations to the portions of the shell on both the suction and pressure surfaces of the blade. It is obvious that the small blade is impractical as shown. A different internal configuration is required, possibly one in which the corrugation amplitude changes along the chord so that the corrugations will contact both shell surfaces. The sketch is shown here only to illustrate some of the problems involved in trying to obtain large internal surface areas in short-chord blades.

Figure 5 shows that in all cases the ratio of heat-transfer surface on the inside of blades to that on the outside can be increased substantially by increasing blade chord (reducing aspect ratio). For very small turbine blades with chords on the order of 0.5 inch, the inside surface area becomes less than the outside surface area. This condition makes cooling the turbine blades extremely difficult.



(a) Turbine diameter, 35 inches.  
(b) Turbine diameter, 25 inches.  
(c) Turbine diameter, 15 inches.

FIGURE 5.—Effect of turbine blade size on inside heat-transfer surface area.



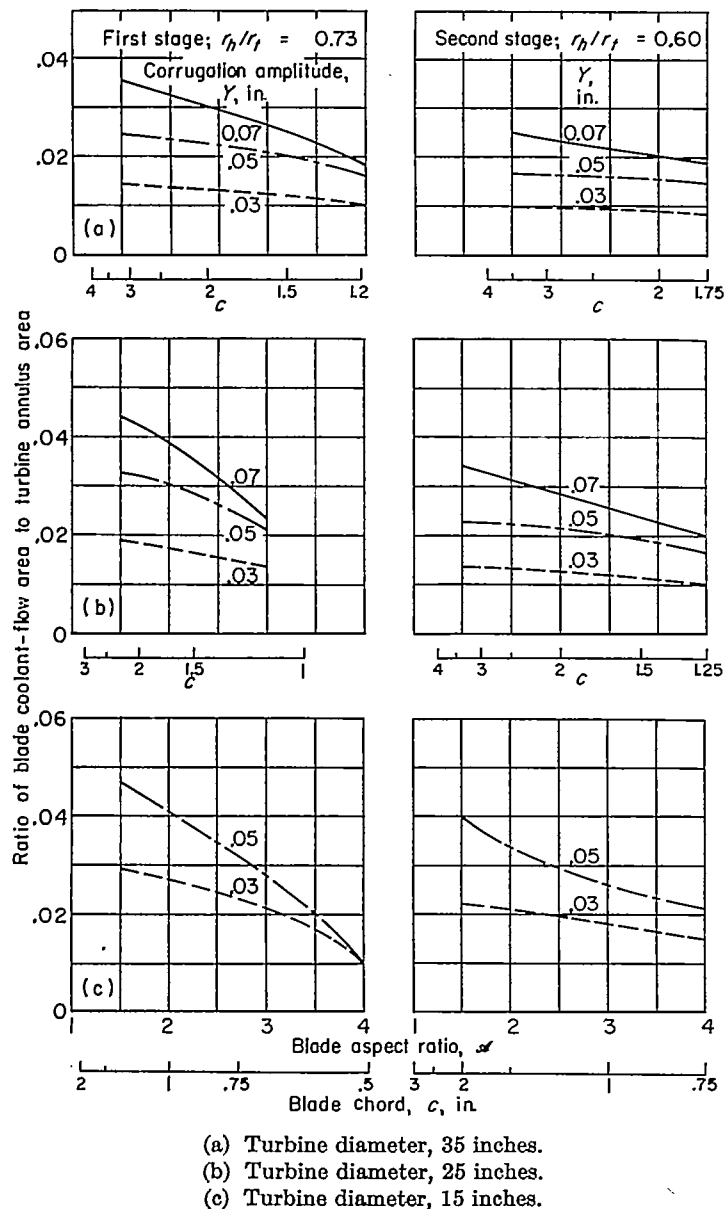


FIGURE 6.—Effect of turbine blade size on coolant-passing flow area.

The corrugation amplitude also affects the amount of surface on the inside of the blade for a fixed corrugation pitch. It should be noted, however, that, with respect to area, frequently a corrugation of 0.07-inch amplitude is little or no better than one of 0.05-inch amplitude. The conduction path is longer with the larger amplitude, and the inside heat-transfer coefficients will be lower for a given mass velocity for the large corrugations, so that the extra heat-transfer surface area with the 0.07-inch-amplitude corrugations does not necessarily result in a blade that requires the smallest quantity of coolant flow. The large amplitude may be advantageous, however, because of large flow area and consequent smaller pressure losses, as is discussed subsequently.

**Coolant-flow area.**—The ratio of the total coolant-flow area in the blades to the gas-flow area in the turbine annulus gives an indication of the quantity of compressor air that

can be bled for turbine cooling for a reasonable pressure drop through the blades; or, conversely, it gives an indication of the pressure losses that will be encountered in the blades for a given coolant-flow ratio. The ratio of blade coolant-flow area to turbine annulus area is plotted in figure 6 as a function of blade chord and aspect ratio, turbine diameter, and corrugation amplitude. The trends here are similar to those for heat-transfer surface area. As the chord is decreased, the coolant-flow area is reduced, which may result in pressure-loss difficulties. It will be noted, however, that large-amplitude corrugations are almost always an advantage as far as coolant-flow area is concerned.

#### BLADE COOLANT-FLOW REQUIREMENTS

**Heat-flow rates.**—The quantity of heat that must be removed from a turbine blade by the cooling air is a function of the gas-to-blade heat-transfer coefficient, the temperature difference between the gas and the blade, and the surface area. The temperature difference between gas and blade is essentially independent of blade chord, since allowable blade temperature is determined by blade stress level (affected only slightly by blade chord) and the stress-rupture properties of the blade material. Also, for constant-solidity turbines the total blade surface area is constant. Consequently, the heat-flow rate into the blade is almost solely a function of the gas-to-blade heat-transfer coefficient  $h_g$ . Equation (15) shows that  $h_g$  varies inversely as the blade chord to the  $1-z$  power.

It is evident, then, that increasing blade chord (or reducing blade aspect ratio) will reduce the cooling loads in blades. This effect is shown on a relative basis in figure 7. As stated previously, it appears that a representative value of  $z$  for rotor blades is 0.70. In reference 11 a value of  $z$  of 0.52 is given for a reaction-type blade that might be suitable for stators. The curves in figure 7 were obtained with these values of  $z$ . The figure shows that doubling the blade chord will reduce the heat-flow rate about 19 percent for rotor blades and about 28 percent for stator blades.

**Required coolant-flow rates.**—The combined effects of the areas shown in figures 5 and 6 and the variations in heat flow illustrated in figure 7 on the coolant flow required to cool blades for the turbines considered in this analysis are

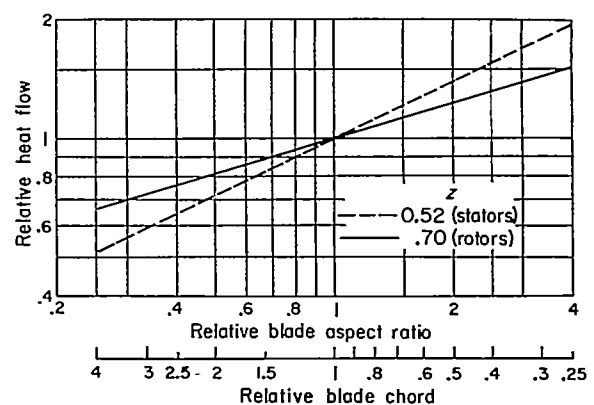


FIGURE 7.—Effect of turbine blade size on heat flow to blade.

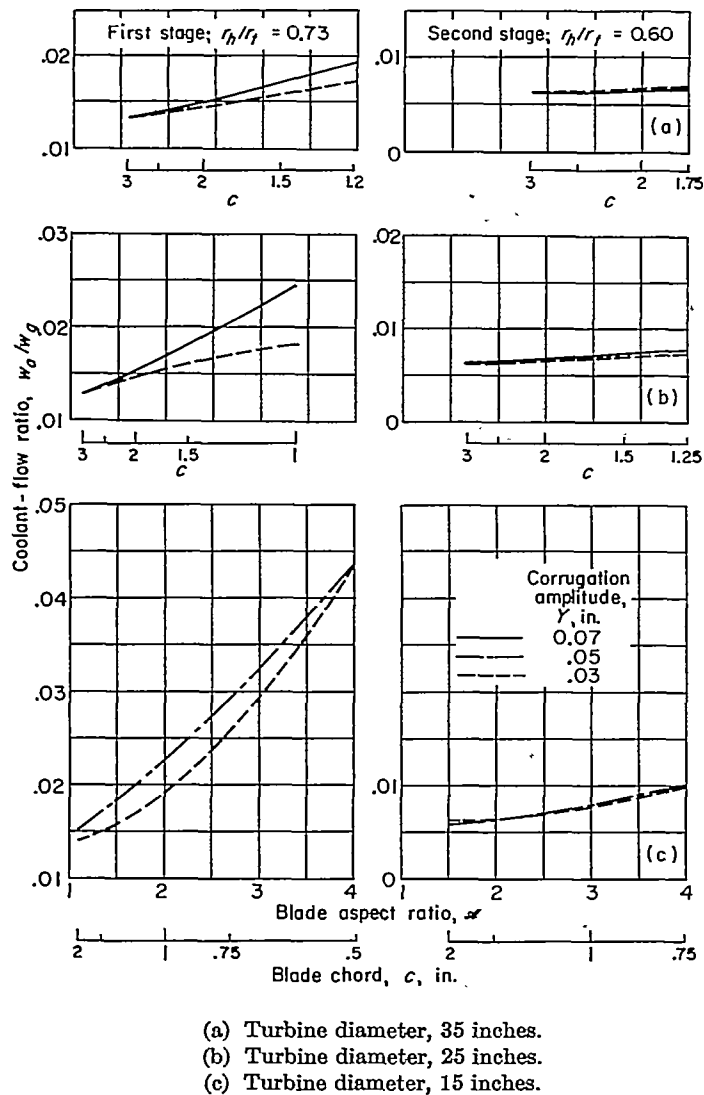


FIGURE 8.—Effect of turbine blade size on coolant-flow requirements.

shown in figure 8, where the ratio of coolant flow to turbine gas flow is plotted against blade chord and aspect ratio. The figure shows that, invariably, as the blade chord is decreased (increased aspect ratio) the total quantity of air required for turbine cooling increases for a given corrugation configuration in the coolant passage. The reasons for this are, of course, obvious from the discussion of previous figures. However, in some cases the variations in required flow rate with blade chord and aspect ratio are quite large, particularly for small turbines, where the chord may become quite small. The analysis shows that the flow required for blades with 1-inch chord is generally about twice that required for blades with 3-inch chord. By further reducing the chord to 0.5 inch, the required coolant flow may become over twice that for blades with a 1-inch chord.

Figure 8 also shows the effect of corrugation amplitude on required cooling-airflow rate. Generally, the effect of amplitude is much smaller than the effect of blade chord on

required coolant flow, particularly for the second stage of the turbines. In the second stage the gas temperature is reduced relative to that of the first stage, so that the cooling load is less severe and smaller variations due to either chord size or corrugation amplitude would be expected. Because of the small effect of corrugation amplitude on cooling-airflow requirements, the required flow for 0.05-inch corrugations is not shown for the 25- and 35-inch-diameter turbines. A few calculations were made, which showed that the flow required for a corrugation of 0.05 inch was intermediate between that required for the 0.07- and 0.03-inch corrugations.

The inside heat-transfer surface area can usually be increased by increasing the amplitude of the corrugations (fig. 5). Large surface area is usually desirable to improve cooling effectiveness, but it will be noted in figure 8 that slightly less cooling air is required with the smaller corrugation amplitude. The larger surface area of the large corrugations is more than offset by the reduced hydraulic diameter (which increases the heat-transfer coefficient) of the small corrugations.

The effect of corrugation geometry on required cooling airflow appears to have a different trend for the 15-inch-diameter turbine than for the other two diameters. For the larger-diameter turbines the difference in required cooling airflows for the 0.07- and 0.03-inch-amplitude corrugations increases with increasing aspect ratio (decreasing chord); but for the 15-inch turbine the required flows are the same for different amplitudes for an aspect ratio of 4. This effect can be explained by the fact that, for a turbine blade with 0.5-inch chord, it was not possible to place any corrugations inside the coolant cavity. For this reason the blade with 0.5-inch chord has the same flow area and same heat-transfer area for the blades represented by both the dashed and the dash-dot lines. The blade was actually a plain hollow blade.

With respect to heat transfer, figure 8 shows that there is generally considerably freedom in the choice of the corrugation amplitude, but pressure losses within the turbine blades should also be considered. Figure 8 gives no indication of the supply pressure required to force the cooling air through the blades. It is possible that under some conditions the pressure available from the engine compressor may be insufficient.

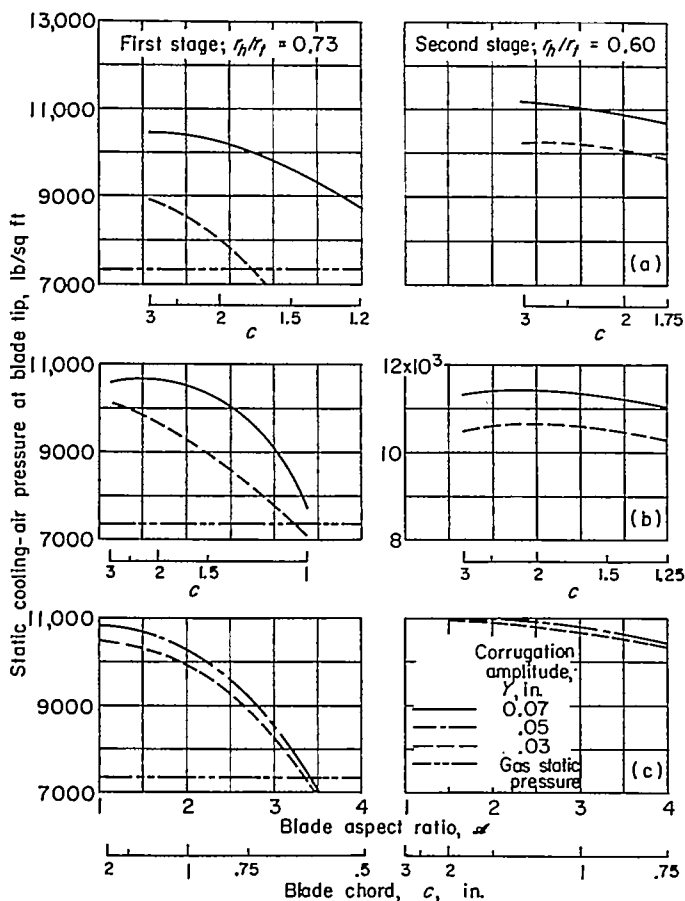
#### BLADE PRESSURE LOSSES

**Coolant pressure at blade tip.**—In order to force coolant through air-cooled turbine blades that discharge the cooling air at the blade tip, it is necessary that the static pressure of the coolant at the tip be at least as high as the static pressure of the gas at the tip. In this analysis coolant pressure losses were calculated for an inlet supply pressure that was as high as is considered feasible with the use of compressor bleed, in order to determine whether it would be possible to force the required flow through the blade. This supply pressure was 90 percent of compressor-discharge total pressure, since it seems likely that at least a 10-percent loss in pressure will result from loss of velocity head and duct losses. The cooling-

air temperature was assumed to be at compressor-discharge temperature. The static pressure of the cooling air at the blade tip is shown in figure 9 for these conditions of inlet pressure and temperature and for the flow rates shown in figure 8. The static gas pressure at the blade tip is also shown for the first stage of the turbine. For the second stage the static gas pressure is not shown, because it is much below the scale on the curves (4000 lb/sq ft, table I).

For all cases shown except one, the static cooling-air pressure at the blade tip in the first stage can become less than the static gas pressure as the blade chord is decreased. This pressure limitation very definitely limits the minimum blade chord that can be tolerated. There appear to be no pressure limitations in the second stage of the turbine.

Figure 9 shows that it may be advantageous to use large-amplitude corrugations in turbine blades to reduce pressure losses, even though the cooling-airflow requirements are somewhat higher (fig. 8). It can be observed from figure 9 that under some conditions it is possible to have a coolant pressure rise through the blades. The supply total pressure to the blades was approximately 9400 pounds per square foot; yet for many cases the tip static pressure is considerably higher than the supply total pressure. This pressure rise is a result of the pumping due to rotation.



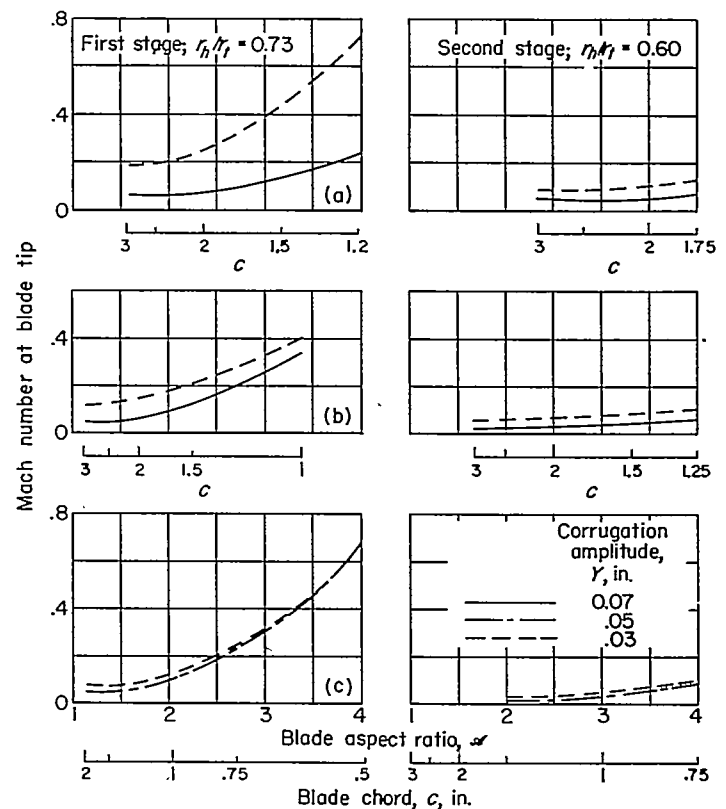
(a) Turbine diameter, 35 inches.  
(b) Turbine diameter, 25 inches.  
(c) Turbine diameter, 15 inches.

FIGURE 9.—Effect of turbine blade size on static cooling-air pressure at blade tip.

Coolant Mach number at blade tip.—Relatively low coolant-passage Mach numbers are generally desirable. High Mach numbers in themselves are not necessarily a disadvantage; but they cause static-pressure losses, and the blades may choke and make it impossible to increase the coolant-flow rate without increasing the coolant density. A high coolant-passage Mach number gives little margin for error in the design. For instance, if the Mach number is 0.7, the flow rate can only be increased about 9 percent for a constant total pressure and temperature before choking will occur. The coolant Mach numbers at the blade tip are shown in figure 10 for the same pressures and flows obtained from figures 8 and 9. Comparison of figures 9 and 10 shows that, when the tip Mach number approaches a value of about 0.4, the static-pressure losses in the blade may become excessive. Figure 10 gives further indication of flow difficulties that can be encountered with small-chord blades.

#### GENERILITY OF RESULTS

The results of this analysis are presented for specific engine conditions. Therefore, the values of blade aspect ratio or blade chord at which cooling may become difficult cannot be considered to be general. By changing the turbine blade material, the coolant temperature, the turbine-inlet temperature, the turbine stress level, the blade stress-ratio factor, or other design conditions, cooling limitations may



(a) Turbine diameter, 35 inches.  
(b) Turbine diameter, 25 inches.  
(c) Turbine diameter, 15 inches.

FIGURE 10.—Effect of turbine blade size on cooling-air Mach number at blade tip.

be met at entirely different conditions from those encountered in this analysis. For example, the cooling-airflow requirements were calculated for the 35-inch-diameter turbine for a chord of 2 inches and a coolant-passage amplitude for three different stress-ratio factors (ratio of design stress to average centrifugal stress). As the stress-ratio factor is increased, the blade is designed for a higher stress level; and consequently it must operate at a lower temperature. As a result, the coolant-flow requirements increase with increasing stress-ratio factor. Figure 11 shows the effect of stress-ratio factor on cooling airflow, tip Mach number, and coolant pressure at the tip. A similar effect would result from varying the blade material. A material capable of withstanding high temperatures might have the trend exhibited for a stress-ratio factor of 1, while a material that could not withstand such high temperatures would exhibit the trends shown for a higher stress-ratio factor. As would be expected, the required coolant flow and tip Mach number increase and tip static pressure decreases with an increase in stress-ratio factor; but there are no great changes that would indicate that the trends of figures previously presented would vary greatly if a different set of conditions were chosen for the calculations. Stress-ratio factor would, of course, have a much larger effect for a blade chord that resulted in higher tip Mach numbers and lower tip static pressures.

Figure 12 shows how coolant-flow requirements, Mach number, and tip pressure can be affected by the coolant temperature. Most of the calculations for this analysis were made with a coolant temperature of 1247° R, which corresponds to the temperature at the discharge of the compressor. By use of an aftercooling device, it may be possible to reduce the cooling-air temperature. In figure 12 curves

are shown for cooling-air supply temperatures of 1247° and 1000° R for the first stage of the 35-inch-diameter turbine. A reduction in cooling-air temperature naturally reduces the quantity of air required for blade-cooling. The cooling-airflow reduction shown in figure 12 varies between about 20 and 25 percent over the range of blade chords investigated. At low coolant Mach numbers the Mach number reduction due to reducing cooling-air temperature is about the same order of magnitude as the reduction in cooling airflow. This effect on static pressure at the blade tip is quite small. For a blade chord of 1 inch, however, there is a large difference in tip Mach numbers owing to the cooling-air temperature effect; but, as can be seen from the shape of the curves, reducing the cooling-air temperature does not allow a significant reduction in permissible blade chord. The results shown in figure 12 are similar to those shown in figure 11, in that the conclusions that can be drawn from this study do not appear to be affected significantly by the value of cooling-air temperature used in the analysis.

It is not within the scope of this report to investigate the effects of turbine blade chord for all combinations of engine conditions. It is believed, however, that enough conditions were investigated to point out trends and to indicate that the use of small-chord blades can become a problem in air-cooled engines. Other blade configurations may possibly create less of a problem than corrugated blades for small chords, but even with those configurations similar trends would be expected. As turbine-inlet temperature is increased above 2500° R, the problems will become more severe than presented herein because of the higher coolant flows that will be required. It can be concluded from this study that in the design of air-cooled turbines it is generally

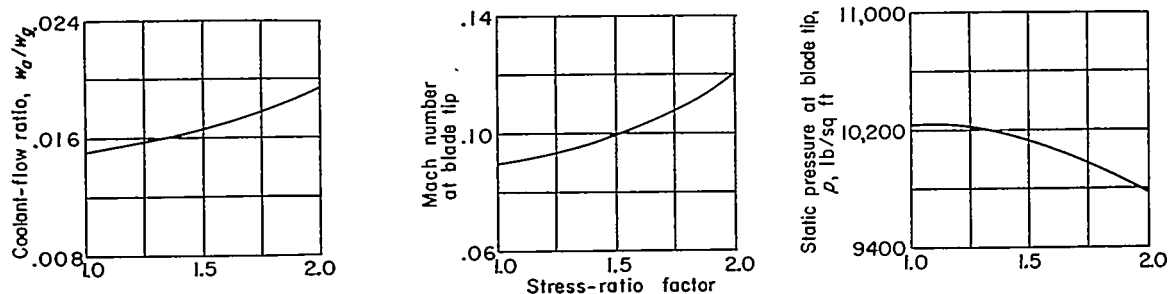


FIGURE 11.—Effect of stress-ratio factor on cooling and pressure-drop characteristics of turbine blades. First stage of 35-inch-diameter turbine; chord, 2 inches; corrugation amplitude, 0.07 inch.

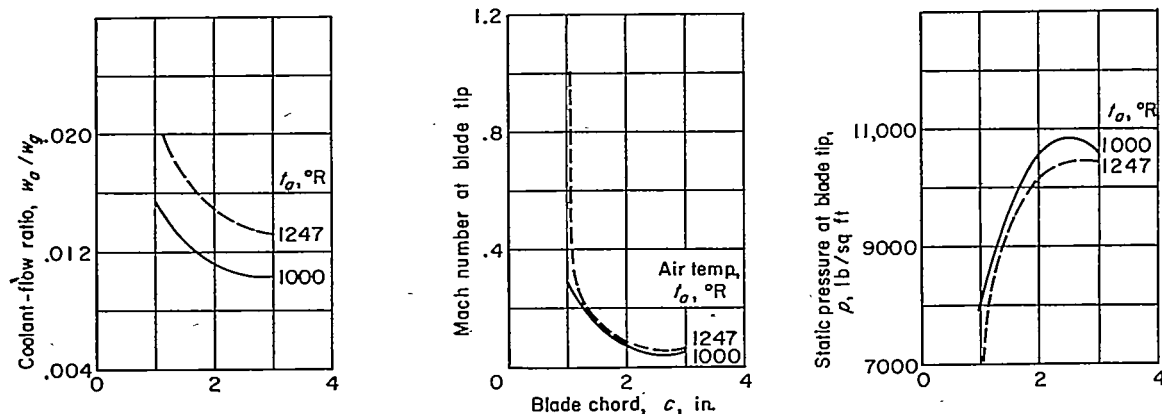


FIGURE 12.—Effect of cooling-air temperature on cooling and pressure-drop characteristics of turbine blades. First stage of 35-inch-diameter turbine; corrugation amplitude, 0.07 inch.

desirable to utilize blades with as large a chord as appears feasible from considerations of disk stress and aerodynamics.

### SUMMARY OF RESULTS

The results of this investigation of the effects of chord size on weight and cooling characteristics of air-cooled turbine blades can be summarized as follows:

1. Air-cooled-turbine blade weight is affected to a much smaller degree by the size of the blade chord than is the weight of solid uncooled blades.

2. When solidity is maintained constant, the heat-transfer surface and the flow area in the coolant passage of air-cooled blades are considerably larger relative to the surface and flow area on the gas side of the blades with large-chord blades than with small-chord blades. As a result, cooling large-chord blades should be easier.

3. Heat-transfer and pressure-drop analyses show that small-chord blades require a larger total amount of cooling air for the turbine and have higher pressure losses than larger-chord blades. Cooling airflow for turbines with 1-inch-chord blades is generally about twice that required for turbines with 3-inch-chord blades. By further reducing the chord to 0.5 inch, the required cooling airflow may become more than twice that for blades with 1-inch chord.

4. Cooling-air pressure losses increase as blade chord is reduced, and it may often be impossible to pass the cooling airflow required at the pressure levels available from compressor bleed to cool blades with small chords.

5. The exact blade chords at which it may no longer be feasible to cool air-cooled blades depend upon the assumptions and conditions of the analysis, but the trends indicated in this report are probably general for other engines, other blade configurations, and other engine conditions.

LEWIS FLIGHT PROPULSION LABORATORY

NATIONAL ADVISORY COMMITTEE FOR AERONAUTICS

CLEVELAND, OHIO, November 13, 1956

### REFERENCES

1. Slone, Henry O., Hubbartt, James E., and Arne, Vernon L.: Method of Designing Corrugated Surfaces Having Maximum Cooling Effectiveness Within Pressure-Drop Limitations for Application to Cooled Turbine Blades. NACA RM E54H20, 1954.
2. Cavicchi, Richard H., and English, Robert E.: A Rapid Method for Use in Design of Turbines Within Specified Aerodynamic Limits. NACA TN 2905, 1953.
3. Esgar, Jack B., and Ziemer, Robert R.: Methods for Rapid Graphical Evaluation of Cooled or Uncooled Turbojet and Turboprop Engine or Component Performance (Effects of Variable Specific Heat Included). NACA TN 3335, 1955.
4. Brown, W. Byron, and Donoughe, Patrick L.: Extension of Boundary-Layer Heat-Transfer Theory to Cooled Turbine Blades. NACA RM E50F02, 1950.
5. Hubbartt, James E., Slone, Henry O., and Arne, Vernon L.: Method for Rapid Determination of Pressure Change for One-Dimensional Flow with Heat Transfer, Friction, Rotation, and Area Change. NACA TN 3150, 1954.
6. Donoughe, Patrick L.: Outside Heat Transfer of Bodies in Flow—A Comparison of Theory and Experiment. M. S. Thesis, Case Inst. Tech., 1951.
7. Kays, W. M., and Clark, S. H.: A Summary of Basic Heat Transfer and Flow Friction Design Data for Plain Plate-Fin Heat Exchanger Surfaces. Tech. Rep. No. 17, Dept. Mech. Eng., Stanford Univ., Aug. 15, 1953. (Contract N6-ONR-251, Task Order 6 (NR-090-104) for Office Naval Res.)
8. McAdams, William H.: Heat Transmission. Second ed., McGraw-Hill Book Co., Inc., 1942.
9. Livingood, John N. B., and Brown, W. Byron: Analysis of Spanwise Temperature Distribution in Three Types of Air-Cooled Turbine Blades. NACA Rep. 994, 1950. (Supersedes NACA RM's E7B11e and E7G30.)
10. Ziemer, Robert R., and Slone, Henry O.: Analytical Procedures for Rapid Selection of Coolant Passage Configurations for Air-Cooled Turbine Rotor Blades and for Evaluation of Heat-Transfer, Strength, and Pressure-Loss Characteristics. NACA RM E52G18, 1952.
11. Hubbartt, James E.: Comparison of Outside-Surface Heat-Transfer Coefficients for Cascades of Turbine Blades. NACA RM E50C28, 1950.

